A025

# 3D FRACTURE CHARACTERIZATION BASED ON GEOMECHANICS AND GEOLOGIC DATA UNCERTAINTIES

Laetitia MACÉ, Laurent SOUCHE and Jean-Laurent MALLET
Nancy School of Geology - Gocad Research Group
BP 40, Avenue du Doyen Marcel Roubault
54501 Vandoeuvre-les-Nancy, France

**Abstract**
*This paper addresses the issue of Naturally Fractured Reservoirs, where fracturation patterns are assumed to be closely related to stress history. Introducing uncertainties on geologic data, we propose to compute a new stochastic parameter, the* ***Failure Probability****, based on geomechanics. This fracture parameter is then used to simulate 3D fracture density and orientation analogue.*

# 1 Introduction

Natural fractures have dramatic effects on reservoirs in term of oil recovery, because they often control the hydraulic flow as conductors (open fractures) or barriers (mineralized fractures). An accurate characterization of fractured reservoirs is needed to build reliable flow models for hydrocarbon exploration. The first step consists in a static modelling of the fracture network geometry as it affects considerably the flow.

Predicting the performance of fractured reservoirs requires the characterization of all fracture parameters such as spacing, orientation, size and aperture. However, none of these fracture attributes is typically well constrained by available subsurface data either because of the restricted number and size of accurate samples (1D wellbores data) or because of the indirectness of measurements (3D seismic data). In [9], Ouenes uses neural networks to identify fracture key parameters, whereas Bourne in [2] proposes to integrate geomechanics in fracture characterization.

Fractures initiation and propagation are mainly due to lithology and local stress distribution (see [7]). In our approach, geologic observations and rock mechanical properties are combined with a fracture geomechanics-based model to predict fracture network attributes. Although the stress field history may only be known after long studies of the field by experts (e.g. regional stress history in [2]), the global stress field can be evaluated through the knowledge of the strain tensor.

Ideally, if the evolution of stress field and the rock failure conditions were precisely known at each point of the subsurface, it would be possible to draw an exact picture of the fracture networks. So, geologic data uncertainties through distribution laws for each rock property are involved into the geomechanic model in order to characterize fracture key parameters. Based on assumptions on the values of mechanical rock properties (cohesion, Young's modulus, etc.) and on their uncertainties, a ***Failure Probability*** is computed across the model. Combined with other fracture drivers, such as seismic attributes and layer thickness, this probability will allow to obtain a **fracture density analogue** that reproduces as well as possible observed well data.

After presenting the theoretical and mathematical basis of this new approach to characterize frac-

ture networks, the stochastic model of fracturation will be detailed. Then, the problem of fracture orientation will be tackled in order to build a reliable geological model.

# 2 Strains and Stresses

Fractures form when rock cannot withstand the in-situ stress anymore and their orientation is constrained by the direction of principal stresses. Fracturation patterns thus highly depend on stress history which is itself related to strain history. The 3D Strain Tensor $\mathcal{E}(\mathbf{x})$ can be obtained at any point in the subsurface through two different methods :

- 3D balanced unfolding of layers (see [5]),
- evaluation of the total deformations in the "Geo-Chronological space" from deposition time to present (see [6]).

The Strain Tensor measures the variations of length of any infinitely small vector $d\mathbf{x}$ at location $\mathbf{x}$. With the Lagrangian Strain Tensor, used later on, elongations are counted negatively while contractions are counted positively.

The eigen values $\{\mathcal{E}_1(\mathbf{x}), \mathcal{E}_2(\mathbf{x}), \mathcal{E}_3(\mathbf{x})\}$ of $\mathcal{E}(\mathbf{x})$ sorted by increasing magnitude order and their associated eigen vectors $\{\mathbf{W}_1(\mathbf{x}), \mathbf{W}_2(\mathbf{x}), \mathbf{W}_3(\mathbf{x})\}$ are called the Principal Strains and Principal Strain Directions at location $\mathbf{x}$, respectively. The forces at the origin of the transformation of the undeformed region $\mathcal{R}_{[0]}$ into the deformed region $\mathcal{R}$ induce a Stress Tensor $\sigma(\mathbf{x})$ whose components can be stored in a $(3 \times 3)$ symmetric matrix $[\sigma(\mathbf{x})]$.

If the material is homogeneous, elastic and isotropic, then, according to the generalized Hooke's law, the Lagrangian Strain Tensor and the Stress Tensor are linked by the following linear equation where $tr([\mathcal{E}(\mathbf{x})])$ represents the trace of $[\mathcal{E}(\mathbf{x})]$ while $\lambda$ and $\mu$ are the so called "Lamé coefficients" characterizing the elastic properties of the material at location $\mathbf{x}$ :

$$[\sigma(\mathbf{x})] \quad = \quad \lambda \cdot tr([\mathcal{E}(\mathbf{x})]) \cdot [I] \; + \; 2\mu \cdot [\mathcal{E}(\mathbf{x})] \tag{1}$$

This equation implies that $[\sigma(\mathbf{x})]$ and $[\mathcal{E}(\mathbf{x})]$ must have the same eigen vectors. The eigen values of $[\sigma(\mathbf{x})]$ and their associated eigen vectors are called, respectively, the Principal Stresses $\{\sigma_i(\mathbf{x})\}$ and the Principal Stress Directions $\{\mathbf{W}_i(\mathbf{x})\}$, where $\mathbf{W}_i$ is also the $i^{th}$ eigen vector of $[\mathcal{E}(\mathbf{x})]$. Still according to the Hooke's law (1), the Principal Strains $\{\mathcal{E}_i(\mathbf{x})\}$ and the Principal Stresses $\{\sigma_i(\mathbf{x})\}$ are linked by the following equation :

$$\sigma_i(\mathbf{x}) \; = \; \lambda \cdot (\mathcal{E}_1(\mathbf{x}) + \mathcal{E}_2(\mathbf{x}) + \mathcal{E}_3(\mathbf{x})) \; + \; 2\mu \cdot \mathcal{E}_i(\mathbf{x}) \qquad \forall\, i \in \{1, 2, 3\} \tag{2}$$

# 3 Failure criteria

Many criteria exist to predict failure of brittle materials. The *Mohr-Coulomb criterion* is appropriate to model shear fractures whereas the *Griffith criterion* is more appropriate in case of tensile failure (see [1]). This paper focuses on shear failure.
The Mohr-Coulomb theory assumes that, for the Principal Stresses such that $\sigma_1 > \sigma_2 > \sigma_3$, the intermediate principal stress component $\sigma_2$ does not act for the failure. It is based on the hypothesis that, between the planes having the same normal stress, the weakest is the one having the maximum tangential stress.

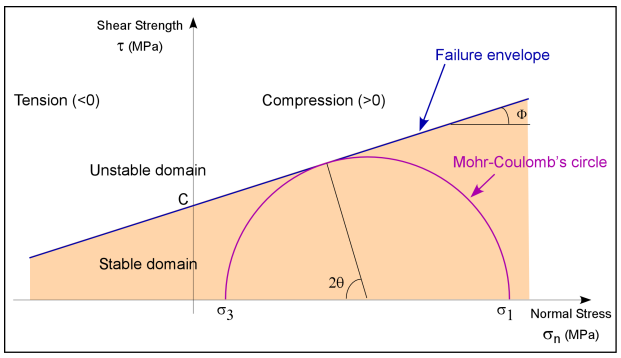


Figure 1: *Mohr-Coulomb's failure criterion. Failure occurs when the Mohr-Coulomb's circle exceeds the failure envelope.*

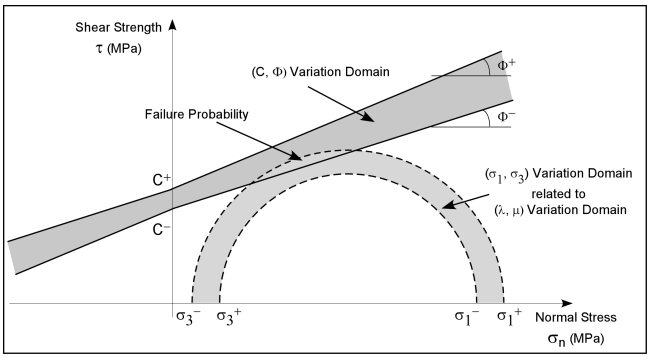


Figure 2: *Mohr-Coulomb's failure criterion including uncertainties on the rock properties $C, \phi, \lambda$ and $\mu$ considered as Uniform probability laws.*

As shown by figure (1), the Mohr-Coulomb's circle is drawn using the maximum principal stress component $\sigma_1$ and the minimum principal stress component $\sigma_3$. The failure envelope is created from Mohr-Coulomb's circles for uniaxial tensile strength and uniaxial compression strength. The Mohr-Coulomb theory states that failure occurs when the Mohr-Coulomb's circle at a point in the subsurface exceeds the failure envelope (see [1]). Using geometric terms and defining $c$ as the intern cohesion and $\varphi$ as the rock friction angle, failure occurs when the distance between the center of the Mohr-Coulomb's circle and the failure envelope is smaller than the radius of the Mohr-Coulomb's circle :

$$\frac{\sigma_1 - \sigma_3}{2} \geq \left| \frac{tg\varphi \cdot \left(\frac{\sigma_1+\sigma_3}{2}\right) + c}{\sqrt{tg^2\varphi + 1}} \right| \tag{3}$$

Assume now, at any point of the subsurface, that the strain tensor $\mathcal{E}$ is perfectly known while the Lamé parameters $\lambda$ and $\mu$, the cohesion $c$ and the friction angle $\varphi$ are realizations of independent random variables $L(\omega)$, $M(\omega)$, $C(\omega)$ and $\phi(\omega)$, respectively. As a consequence, fracturation must now be considered as a random event and it makes sense trying to evaluate its probability to occur when $\mathcal{E}$ is known and the probability laws of $L(\omega)$, $M(\omega)$, $C(\omega)$ and $\phi(\omega)$ are given (see figure (2)).

# 4 A Stochastic Model of fracturation

According to equation (3), it can be observed that :

$$\{\text{fracturation occurs}\} \iff c \leq \frac{\sigma_1 - \sigma_3}{2} \cdot \frac{1}{cos\varphi} - \frac{\sigma_1 + \sigma_3}{2} \cdot tg\varphi \tag{4}$$

The Principal Stress Components $\sigma_1$ and $\sigma_3$ of the stress tensor are deduced from the Principal Strain Components $\mathcal{E}_1$, $\mathcal{E}_2$ and $\mathcal{E}_3$ of the strain tensor $\mathcal{E}$ through the generalized Hooke's law (see equation (2)). Let $h(\lambda, \mu, \varphi|\mathcal{E})$ be the function defined by :

$$h(\lambda, \mu, \varphi|\mathcal{E}) = (\mathcal{E}_1 - \mathcal{E}_3) \cdot \mu \cdot \frac{1}{cos\varphi} - (\mathcal{E}_1 + \mathcal{E}_3) \cdot \mu \cdot tg\varphi - (\mathcal{E}_1 + \mathcal{E}_2 + \mathcal{E}_3) \cdot \lambda \cdot tg\varphi \tag{5}$$

Using equations (4) and (5), it can be concluded that fracturation is characterized by the following equation :

$$\{\text{fracturation occurs}\} \iff c \leq h(\lambda, \mu, \varphi|\mathcal{E}) \tag{6}$$

In practice, the properties $(\lambda, \mu, c, \varphi)$ of the material at a given location in the subsurface are not know with precision. As a consequence, to characterize the fracturation in the subsurface, it may be wise to use the stochastic model presented in the following.

**Stochastic model of fracturation**

Knowing the strain tensor $\mathcal{E}$ and the probability laws of $L(\omega)$, $M(\omega)$, $C(\omega)$ and $\phi(\omega)$ at any point of the subsurface, the *Failure Probability* $PF_{CLM\phi}(\mathcal{E})$ is defined as :

$$PF_{CLM\phi}(\mathcal{E}) \;=\; I\!P(\ \{\omega \in \mho \;:\; \text{fracturation occurs}\}\ ) \quad \text{where } (\mho, \mathcal{A}, I\!P) \text{ is a probabilized space.} \tag{7}$$

According to equations (6) and (7) and defining $F_C$ as the Cumulative Distribution Function (cdf) of the random variable $C(\omega)$, it can be observed that :

$$I\!P\Big(\ \{\omega \in \mho \;:\; \text{fracturation occurs}\}\ \&\ \{L(\omega) = \lambda\}\ \&\ \{M(\omega) = \mu\}\ \&\ \{\phi(\omega) = \varphi\}\ \Big) \;=\; F_C(\ h(\lambda, \mu, \varphi|\mathcal{E})\ ) \tag{8}$$

Taking into account the independence of the random variables $L(\omega)$, $M(\omega)$, and $\phi(\omega)$, the probability for fracturation to occur can be computed as follows :

$$PF_{CLM\phi}(\mathcal{E}) \;=\; \int_{I\!R^3} F_C(\ h(\lambda, \mu, \varphi|\mathcal{E})\ )\ \cdot\ f_L(\lambda) \cdot f_M(\mu) \cdot f_\phi(\varphi)\ \cdot\ d\lambda\, d\mu\, d\varphi \tag{9}$$

In practice, the kernel of the integral (9) is not convenient to be integrated analytically and the use of a numerical integration technique is far more practical to evaluate the failure probability $PF_{CLM\phi}(\mathcal{E})$. Two cases have been studied for the computation of the *Failure Probability* : one when the distribution laws of the random variables are considered to be Gaussian probability laws (Gauss-Hermite quadrature technique) and the other for Uniform probability laws (Legendre quadrature technique). In the following, the results are detailed.

# 5 Test case

In order to validate the results obtained with both numerical methods (Gaussian and Uniform probability laws), a synthetic case and a geological case have been studied. In both models, the material is assumed to be a homogeneous layer of sandstone and assumptions on the elastic properties of the rock and on their uncertainties have been made from the well-known geomechanics referenced books of Goodman [3] and Jaeger [4].

**Synthetic case**

This case concerns the flexure of a sedimentary layer. As the thickness of the layer is small compared to its extension, the elastic theory of thin plates can be applied (see [14]). The "Lagrangian Strain Tensor" $\mathcal{E}(\mathbf{x})$ has been deducted analytically from the parametric representation of the thin plate (see [12]). In our case, the neutral surface has been placed at the bottom of the thin plate. The *Failure Probability* has been computed on this model for Gaussian and Uniform distribution law types as shown by figure (4). The results of both numerical techniques are very similar and the difference between the methods is inferior to 2 percent. Both results are also geologically consistent : below the white region, strains resulting from the stress field are not major to generate sets of fractures, while the strains acting in the red region are more likely to provide fracture networks.

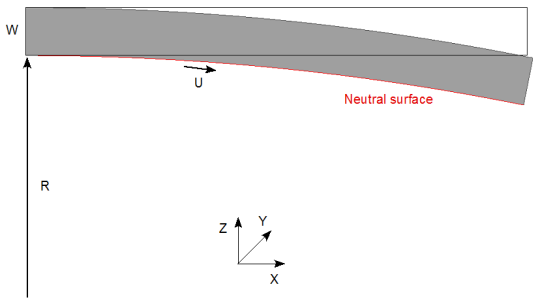


Figure 3: *Cross-section of a bent elastic thin plate (R=1000; W=20).*

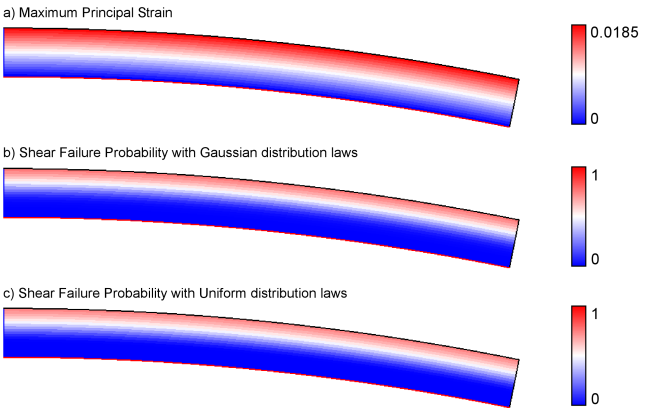


Figure 4: *a) Maximum Principal Strain computed analytically on a deformed thin plate. Comparison of Failure Probabilities on a thin plate when all properties distribution laws are Gaussian (b) or Uniform (c).*

## Geological case

Tests have also been performed on the geological anticline of Split Mountain in Utah (USA), which is composed of a unique homogeneous layer. To obtain the "Lagrangian Strain Tensor", a 3D balanced unfolding has been performed (see [5]). Then, the *Failure Probability* has been computed still with both methods : Gaussian and Uniform distribution laws. As shown by figure (5), the results are also very similar between both numerical approaches (difference between methods is less than 5 percent). As expected, the *Failure probability* is higher on the top of the anticline where the extensions forces are maximal, while it is lower for other less deformed regions.

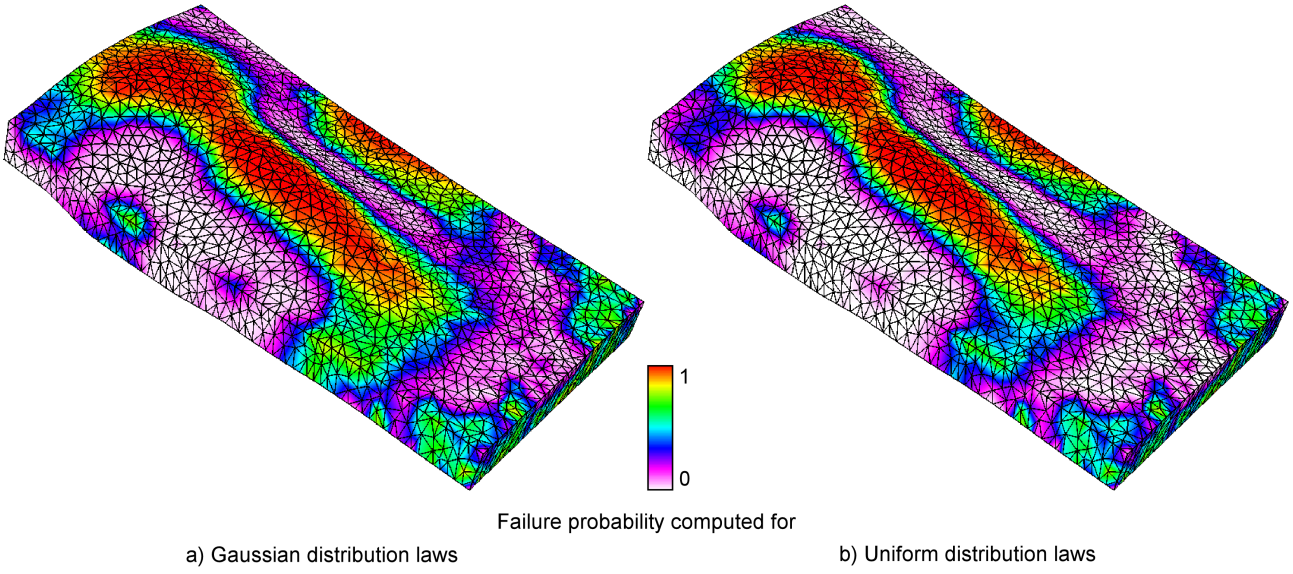


Figure 5: *Comparison of Failure Probabilities on a geological case (Split Mountain) when all properties distribution laws are Gaussian (a) or Uniform (b).*

**Comparison with Curvature results**

Another common technique used to predict fracture characteristics is the computation of curvatures as in [10]. Curvatures of horizons are used to compute an ”index of occurrence of fractures” playing the same role as our *Failure Probability*. However, there are some severe drawbacks with such an approach :
1) Curvatures on surfaces are characterized by 2D tensor while Strain Tensor is 3D: as a consequence, there is no direct mathematical connection between these two tensors.

2) In the case of an isopach fold, the top and bottom horizons have the **same** curvature. However, the top is in extension while the bottom is in compression. In such a case, the ”index of occurrence of fractures” based on curvatures will be the same while the *Failure Probability* will be **extremely different**. Figure (6) shows a cross-section of the Split Mountain anticline : the *Failure Probability* is higher on top of the anticline which corresponds to usual observations on outcrops while the curvature does not give any similar information (dissymmetry of the curvature property is due to the dissymmetry of the 3D structure of the anticline).

3) Curvatures cannot take into account rock types. As a consequence, in a folded stack of alternate isopach layers of carbonates and shales, for example, both rock types will be assigned the same ”index of occurrence of fractures” which is not the case for the *Failure Probability*.

4) Finally, from a mechanical point of view, the direction of fractures can be determined correctly only if the 3D Strain Tensor is known : the 2D Curvature Tensor cannot provide such an information.

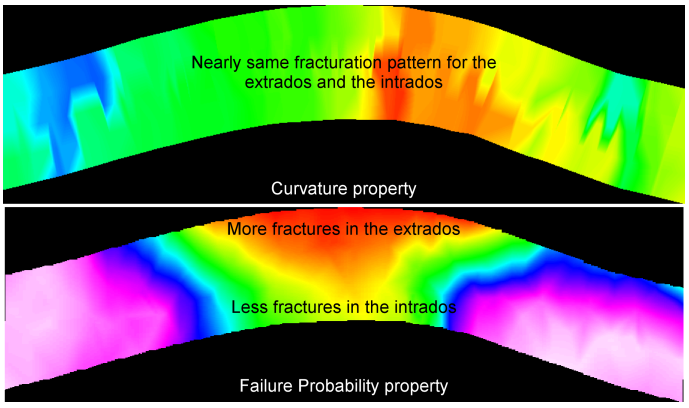


Figure 6: *Comparison of Curvature and Failure Probability properties for a N-S cross-section at the maximum of the Split Mountain anticline.*

# 6 Fractures Orientation

Tectonic fractures are those whose origin, on the basis of orientation, distribution, and morphology, is attributed to, or associated with, a local tectonic event. They are formed by the application of surface forces. In [8], Nelson has observed that the majority of tectonic fractures in outcrop tend to be shear fractures. Shear fractures have a sense of displacement parallel to the fracture plane. At a point **x**,

they form at some acute angle to the maximum compressive principal Stress Direction $\mathbf{W}1(\mathbf{x})$ and at an obtuse angle to the minimum compressive Stress Direction $\mathbf{W}3(\mathbf{x})$ within the rock. They form parallel to the intermediate compressive Stress Direction $\mathbf{W}2(\mathbf{x})$. All three principal stresses must be compressive for shear fractures formation.

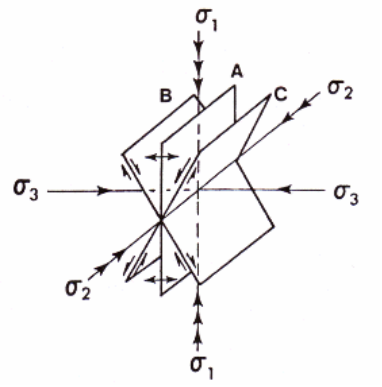


Figure 7: *Potential fracture planes developed in laboratory compression tests. Extension fractures (A) and shear fractures (B and C) are shown. After Nelson (2001).*

As presented in section (2), the intermediate Stress Direction $\mathbf{W}_2(\mathbf{x})$ are known in the undeformed space (both methods of computation for the strain eigen vectors can be used, either a 3D balanced unfolding [5] or the Geochron model [6]). Then fracture orientation can easily be determined in the undeformed space as shown by figure (8a). Finally, a transformation from the undeformed space to the deformed space allows to represent fracture orientation in the deformed space (see figure (8b)).

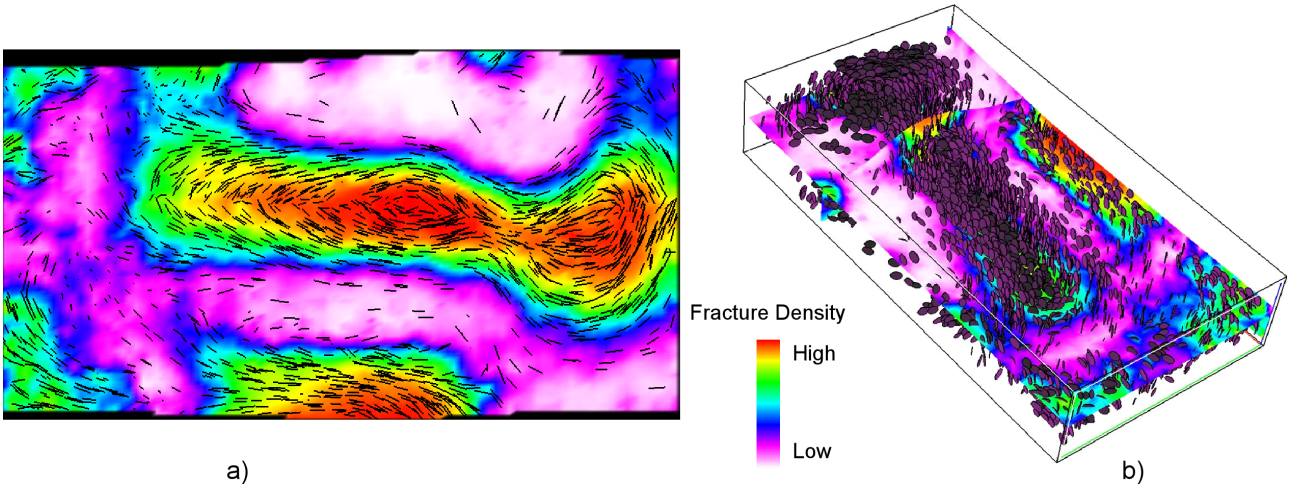


Figure 8: *Fracture orientation. a) Discrete Fracture Networks simulated in the undeformed space, Top view (fractures are the black lines). b) Previous simulation transformed to the deformed space, Side view. In both pictures, the displayed property on cross-sections is the fracture density.*

# Conclusion and Future Works

Data uncertainties have been integrated into the geomechanics concepts in this approach of fracture characterization. A new parameter, the *Failure Probability*, has been computed in order to take into

account the elastic rock properties and the stress field constraining the material for fracture density assessment. Using a non-linear multi-regression, this probability is combined with other fracture drivers, such as seismic attributes and layer thickness, to obtain a fracture density analogue that reproduces as well as possible observed well data. The geomechanical parameters are also used to determine fracture orientation, a future work about fracture orientation estimation will be to integrate a stochastic information from the failure criterion. The next investigation of this fracture parameters study is about fracture size and aperture in order to simulate Discrete Fracture Networks as described by Souche in [13], and also to deal with tensile fracturation pattern. The obvious final step will then be the assessment of an equivalent permeability of the fractured media.

## Acknowledgments

This research work was performed in the frame of the gOcad research project. The companies and universities members of the gOcad consortium are hereby acknowledged. The support of the Carfrac Consortium, and especially IFP, who provided the Split Mountain data set is also gratefully acknowledged.

# References

[1] Blès, J-L. and Feuga, B., (1996). *La Fracturation des Roches,* Editions du B.R.G.M., Orléans, 121p.

[2] Bourne, S., Brauckmann, F., Rijkels, L., Stephenson, B., Weber, A., and Willemse, E., (2000). *Predictive Modelling of Naturally Fractured Reservoirs using Geomechanics and Flow Simulation,* In Proceedings of the 9th ADIPEC.

[3] Goodman, R. E., (1989). *Introduction to Rock Mechanics,* John Wiley & Sons, New York, 576p.

[4] Jaeger, J.C., (1969). *Elasticity, Fracture and Flow, with Engineering and Geological Applications,* 3rd edition Methuen, London, 268p.

[5] Mallet, J.L., (2002). *Geomodeling,* Oxford University Press, New York, 600p.

[6] Mallet, J.L., (2004). *Space-Time Mathematical Framework for Sedimentary Geology,* Mathematical Geology, 36, No.1, 32p.

[7] National Research Council, (1996). *Rock Fractures and Fluid Flow: Contemporary Understanding and Applications,* National Academy Press, Washington D.C., 551p.

[8] Nelson, R.A., (2001). *Geologic Analysis of Naturally Fractured Reservoirs,* Gulf Professional Publishing, 2nd edition, Houston, 320p.

[9] Ouenes, A., (2000). *Practical Application of Fuzzy Logic and Neural Networks to Fractured Reservoir Characterization,* Computer and Geosciences, 26, 953-962.

[10] Ozkaya, S.I., (2002). *CURVAZ - a program to calculate magnitude and direction of maximum structural curvature and fracture-flow index,* Computer and Geosciences, 28, 399-407.

[11] Press, W.,H., Teukolsky, S.A., Vetterling, W.,T., Flannery, B.,P., (1992). *Numerical Recipies in C,* Cambridge University Press, 994p.

[12] Royer, J.J., Cognot, R., Moyen, R., Mallet, J.L., (2003). *Deformation and Fracturation in GOCAD,* In Proceedings of the 23th Gocad Meeting,29p.

[13] Souche, L., Macé, L., (2003). *Discrete Fracture Network Modelling : Perpectives,* In Proceedings of the 23th Gocad Meeting,18p.

[14] Turcotte, D. and Schubert, G., (1982). *Geodynamics: Application of Continuum Physics to Geological Problems,* John Wiley & Sons, New-York, 464p.